Poly((*N*,*N*,*N*-trimethylammonio)ethyl acrylate chloride salt) (PCMA)−SDS Complex Formation in Dilute Aqueous Solution. Light Scattering and Time-Resolved Fluorescence Quenching Measurements

Johan Fundin, Wyn Brown,* and Martin Swanson Vethamuthu

Department of Physical Chemistry, University of Uppsala, Box 532, 751 21 Uppsala, Sweden

Received April 14, 1995; Revised Manuscript Received November 2, 1995[⊗]

ABSTRACT: This paper describes changes in the cationic polyelectrolyte PCMA coil conformation when the anionic surfactant SDS is added in the presence of a simple salt. Four different SDS/PCMA mass concentration ratios (0.074, 0.149, 0.223, and 0.298, corresponding to 0.05, 0.10, 0.15, and 0.20 molar concentration ratios, respectively) have been examined at different NaCl concentrations. Higher ratios than the above give precipitation. When the polyelectrolyte−surfactant complex is formed, the hydrodynamic radius, R_h, is smaller than that for the pure polymer as a result of a combination of electrostatic and hydrophobic interactions. The decrease in R_h on addition of SDS to the PCMA/NaCl solutions is strong even at these low ratios. Inverse Laplace transformation (ILT) of the autocorrelation functions showed that at low salt concentrations there are two modes corresponding to the presence of aggregates (clusters) and the single-coil polymer−surfactant complex. The slow component is distinguished from the analogous component in the earlier studied NaPSS−CTAB system for which the relative intensity of the cluster mode increases strongly on addition of a simple salt. Static light scattering results in 100 mM NaCl show a decrease in the radius of gyration, R_g, as the SDS concentration is increased, in agreement with the observed changes in R_h. The concomitant decrease in the second virial coefficient, A_2, when the surfactant/polyelectrolyte ratio is increased, reflects the reduction in the interaction potential when the complex approaches precipitation. Aggregation numbers, N_s, for the bound SDS micelles were measured at different SDS/PCMA ratios in 50 and 100 mM NaCl using time-resolved fluorescence quenching. All measurements resulted in higher N_s values than those for SDS in the absence of PCMA at the same concentration of NaCl.

Introduction

Considerable interest has developed in polymer−surfactant systems in the last two decades, both as regards technical applications and in fundamental biochemistry. The most well-studied systems have been solutions of a neutral polymer and negatively charged surfactant, e.g. poly(ethylene oxide) (PEO)−sodium dodecyl sulfate (SDS).[1−5] Three different domains exist in the phase diagram for this system.[6−8] In the first, free polymer chains and surfactant molecules are present in the solution. Polymer−surfactant interaction is a feature of the second in which most of the surfactant is bound in micellar form to the polymer. Above saturation in domain three, free micelles and PEO−SDS complexes coexist. It is widely accepted that micellization of SDS is facilitated by the presence of PEO, resulting in a substantially lower critical aggregation concentration, cac, compared to the cmc, with a correspondingly lower aggregation number. Changes in the aggregation number of the surfactant in the presence of PEO measured by fluorescence decay[9] also demonstrate that PEO−SDS interactions occur. The conformation of the PEO−SDS complex differs from that of pure PEO in aqueous solution owing to the presence of the SDS micelles fixed along the chain backbone. Thus, both R_h and the intrinsic viscosity of the complex increase strongly as the SDS concentration is increased as a result of the electrostatic repulsion between the small charged micelles fixed on the PEO chain. The interaction potential between the bound micelles of course depends strongly on the concentration of simple salt owing to screening effects. With excess surfactant, the interaction potential between the fixed micelles becomes progressively screened and leads to a decrease, for example, in the coil radius and the solution viscosity. The maximum in the PEO coil extension corresponds to a mass concentration ratio SDS/PEO ≈ 5, in 100 mM NaCl, and this is also reflected in the virial dependence of the diffusion coefficient of the complex. Above this concentration ratio, free micelles first appear in the solution. An initial increase in viscosity with increasing surfactant concentration is the usual behavior in these kinds of system. However, the (ethylhydroxy)ethyl cellulose (EHEC)−SDS system[10] exhibits a reduction in the viscosity at dilute polymer concentrations, which is explained by intrachain coupling through surfactant molecules. This cellulose derivative is relatively hydrophobic, leading to attractive interactions between the polymer chains. The associative interaction is reinforced on addition of SDS, giving a pronounced change in the conformation of the polymer molecules and a hydrodynamic volume which is 4 times smaller than that in the absence of SDS. With regard to the interaction between negative polyelectrolytes and positive surfactants, the system sodium poly(styrenesulfonate) (NaPSS) and alkyltrimethylammonium halide surfactants is one of the best studied.[11−13] There is strong electrostatic association between this polyelectrolyte and the oppositely charged surfactant, leading to irreversible phase separation above the point at which the polyelectrolyte is saturated with surfactant. This is one of the most conspicuous differences compared to the neutral polymer−ionic surfactant systems. The solubility of the polyelectrolyte−surfactant complex is dependent on a minimum charge density along the chain backbone

[⊗] Abstract published in *Advance ACS Abstracts,* January 15, 1996.

0024-9297/96/2229-1195$12.00/0

which in the CTAB/NaPSS system corresponds to about 68% charge neutralization in terms of the molar concentration ratio. The cac is much lower than the cmc, and the binding of the cationic surfactant to the anionic polymer is cooperative. The reason for the cooperativity is the electrostatic stabilization of the micelles which in turn depends on the charge density, flexibility, and hydrophobic character of the polyion chain. Another pronounced difference between this system and a neutral polymer−negative surfactant system is the strong dependence of the thermodynamic interaction parameter, k_D, on the surfactant concentration which is due to a reduction of the complex charge density with increased surfactant concentration, and a corresponding decrease in the interaction potential.

The precipitation point in systems containing highly charged polymer−surfactant complexes can be changed by introducing ionic−nonionic mixed micelles into the solution. Dubin and Oteri[14] studied the association between the strong polycation poly(dimethyldiallylammonium chloride) (PDMDAAC) and SDeS−Triton X-100 mixed micelles. It was found that phase separation depends on the ionic strength and the mole fraction of the anionic surfactant SDeS, but is relatively insensitive to the concentrations of polyelectrolyte and total surfactant. The binding of poly(styrenesulfonate) to mixed cationic−zwitterionic surfactant micelles has also been studied using deuterium NMR[15] in a system containing mixed micelles of cationic CTAB and zwitterionic hexadecylphosphocholine. The deuteron labels locate in the polar headgroup of the zwitterionic surfactant. Addition of NaPSS to a solution with CTAB−HDPC-γ-d_6 mixed micelles showed a concentration-dependent precipitation behavior, a dependence which diminishes on reduction of the micellar surface charge density or by increasing the simple salt concentration. The reduction in intensity of the deuterium NMR spectrum of CTAB−HDPC-γ-d_6 mixed micelles when NaPSS is added, and a recovered intensity at higher polyelectrolyte concentrations, correlates with the precipitation of the complexes and their subsequent resolubilization.

This paper describes a light scattering study of the strong association between the polycation PCMA and the anionic surfactant SDS in dilute aqueous solution, in which the physical and dynamical properties of the PCMA−SDS complex and higher order aggregates are examined. Light scattering measurements are complemented by time-resolved fluorescence quenching and surface tension measurements to characterize the properties of the micelles bound to the polyelectrolyte. From the aggregation numbers of the bound micelles, the number of micelles per chain at different SDS/PCMA ratios in 100 mM NaCl has been estimated. All measurements were made at 25 °C.

Experimental Section

Poly((*N*,*N*,*N*-trimethylammonio)ethyl acrylate chloride salt) (Figure 1) with a reported molecular weight $M_w = 1.6 \times 10^6$ was synthesized at Laboratoire de Physico-Chimie Macromoléculaire, Université Pierre et Marie Curie, Paris.[16] This polyelectrolyte is 100% ionizable and has a linear charge density characterized by one charge per segment with a length 0.27 nm. The anionic surfactant SDS from BDH Laboratory Supplies, Poole, U.K., was used without further purification but was shown to be of high purity by the agreement of its cmc with the established literature value 8.3 mM[17] in pure water. Milli-Q grade water from a Millipore apparatus was used for sample preparation. After reaching equilibrium, the solutions were filtered through 0.2 μm Sartorius Minisart N filters, into cylindrical glass light scattering cells of 15 mm diameter. Regarding the fluorescence quenching measurements, pyrene (Aldrich), was recrystallized twice from ethanol and dimethylbenzophenone (DMBP, Aldrich) with purity >99% was used as supplied.

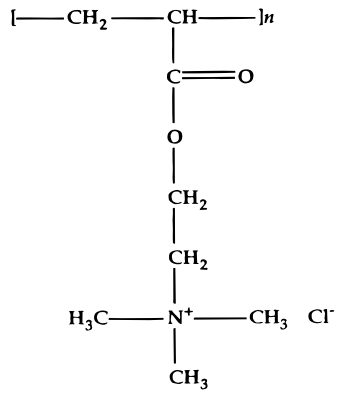

Figure 1. Structure of poly((trimethylammonio)ethyl acrylate chloride salt) (PCMA).

Polyelectrolyte−Surfactant Solutions. Solutions containing 0.2% PCMA with NaCl were titrated using a buret with an equal volume of SDS solution containing NaCl, where the SDS concentrations were 0.015, 0.030, 0.045, and 0.060%, respectively. Stirring was thereafter continued for at least 24 h to attain equilibrium. The mixture was diluted and filtered into the glass light scattering cells. For static light scattering measurements the solutions were dialyzed using a membrane, with 2.5 nm pore size, from Union Carbide Corp., Chicago.

In the preparation of the PCMA−SDS samples for fluorescence measurements a stock solution of pyrene and the quencher DMBP in ethanol was used. To introduce the probe into the sample, an appropriate amount of the stock solution was placed in a volumetric flask and the solvent evaporated by passing a gentle stream of nitrogen over it. The pyrene was then solubilized into the PCMA−SDS solution by stirring. The pyrene concentration was kept low enough ($<10^{-7}$ M) to prevent excimer formation. DMBP was similarly introduced into a part of the polyelectrolyte−surfactant solution with probe to give a single concentration of probe, quencher, and surfactants. All solutions were thoroughly stirred mechanically for more than 4 h until the probe and quencher were completely solubilized and then allowed to stand sufficiently long to ensure equilibrium conditions. All samples were deoxygenated by freeze−thaw cycles at least three times under vacuum in special quartz cuvettes prior to the fluorescence measurements.

Dynamic Light Scattering (DLS). The technique and apparatus used were those described in ref 18. An ALV 5000 wide-band multi-τ digital autocorrelator from ALV-Langen, Germany, was employed to determine the relaxation time distribution. This instrument has a monitoring capacity of up to nine decades in delay time. The measured time intensity correlation function is related to the electric field correlation function by the Siegert relation:

$$g^{(2)}(t) = B(1 + \beta|g_1(t)|^2) \quad (1)$$

where B is a baseline and β is a factor which takes into account deviations from ideal correlation, for instance fluctuations in the scattering volume. In a continuous distribution corresponding to an infinite range of particle sizes, ILT was used:

$$g^{(1)}(t) = \int_0^\infty A(\tau) \exp(-t/\tau)\, d\tau \quad (2)$$

ILT was performed by using a constrained regularization routine, REPES, developed by Jakeš,[19] to obtain the distribution of decay times. This program is similar in many respects to CONTIN, developed by Provencher,[20] but directly minimizes the sum of squared differences between the experimental and calculated intensity−intensity correlation functions, $g^{(2)}(t)$, using nonlinear programming and allows selection of the

parameter P (probability to reject), which determines the degree of smoothing. The analysis of data, encompassing 288 exponentially spaced grid points and a grid density of 12 per decade can be rapidly performed on an IBM-AT desk-top computer. Relaxation time distributions are given in the form $\tau A(\tau)$ versus log τ, providing an equal area representation. Diffusion coefficients are calculated from the ILT moments as $D = (\Gamma/q^2)_{q\to 0}$, where Γ is the relaxation rate and q is the magnitude of the scattering vector.

Static Light Scattering (SLS). Measurements were carried out by using a Hamamatsu photon-counting apparatus, with a 3 mW helium−neon laser (633 nm). Toluene (Rayleigh ratio 13.59×10^{-6} cm^{-1}) was used in the calibration.[21] R_g and A_2 for the polyelectrolyte and for the complex were calculated in 100 mM NaCl and for SDS/PCMA molar ratios 0.05, 0.10, and 0.15. The concentration dependence of the particle form factor and the angular dependence of A_2 is illustrated in Zimm plots. The total intensity was measured over a wide range of angles for each concentration to obtain R_g with good precision. Since the measured intensity is the integrated quantity, SLS measurements were made on the solutions corresponding to single modal relaxation time distributions for the complex to minimize contributions from aggregates.

Time-Resolved Fluorescence Quenching (TRFQ). Time-resolved fluorescence decay data were collected with the single photon counting technique, as described earlier.[22] The excitation wavelength was 323 nm, and the pyrene monomer emission was measured at 395 nm. The TRFQ measurements were performed at 25 °C. The fluorescence quenching data were fitted to a generalized model for fluorescence deactivation proposed by Infelta et al.[23] The generalized equations used in the analysis are the following:[24]

$$F_t = A_1 \exp[-A_2 t + A_3(\exp(-A_4 t) - 1)] \tag{3}$$

where the expression for the parameters A_1 to A_4 are given by

$$A_1 = F_0 \tag{3a}$$

$$A_2 = k_0 + k_q\langle x\rangle_s \tag{3b}$$

$$A_3 = \langle n\rangle\left(1 - \frac{\langle x\rangle_s}{\langle n\rangle}\right)^2 \tag{3c}$$

$$A_4 = \frac{k_q}{\left(1 - \frac{\langle x\rangle_s}{\langle n\rangle}\right)} \tag{3d}$$

where F_0 is the fluorescence intensity at time $t = 0$, k_0 is the first-order decay constant, $k_0 = 1/\tau_0$, $\langle x\rangle_s$ is the average number of quenchers in micelles with a surviving excited probe during the stationary part of the fluorescence decay, and $\langle n\rangle$ is the average number of quenchers in a micelle. The aggregation number, N_s, is easily obtained from

$$N_s = \frac{\langle n\rangle S_m}{Q_m} \tag{4}$$

where S_m and Q_m are the concentrations of the aggregated surfactant and quenchers in the micellar phase. Equation 3 has the same form as the Infelta−Tachiya equation,[23,25] but the expressions for the parameters A_1 to A_4 differ. In the Infelta−Tachiya case

$$\frac{\langle x\rangle_s}{\langle n\rangle} = \frac{k_-}{k_q + k_-} \tag{5}$$

and eq 3 reduces to the parameters in the Infelta case. The natural lifetime of pyrene, τ_0, was determined in separate experiments without quencher. In order to handle the effect of a short-lived fluorescing species in the polyelectrolyte−surfactant solution which perturbed the initial part of the decay, modified version of eq 3 was used, which contained

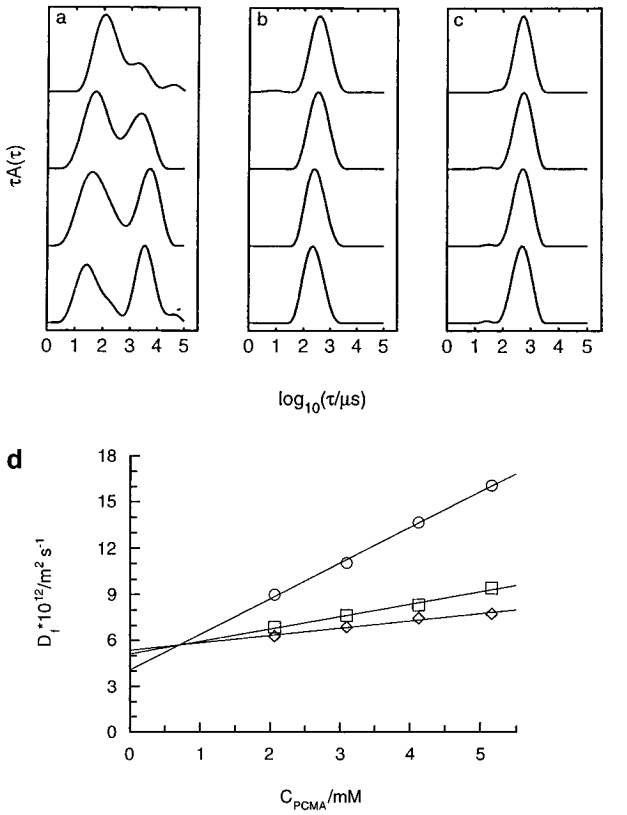

Figure 2. (a−c) Relaxation time distributions of PCMA. Concentrations of the polycation from top to bottom are 2.07, 3.10, 4.13, and 5.16 mM, in (a) 1 mM NaCl, (b) 10 mM NaCl, and (c) 100 mM NaCl. (d) Effective diffusion coefficient, D, of PCMA for the fast relaxation mode plotted versus PCMA concentration in 10 mM (○), 50 mM (□), and 100 mM NaCl (◇).

terms representing the weighted contribution of the perturbant.

$$F_t = A_1 \exp[-A_2 t + A_3(\exp(-A_4 t) - 1)] + F_{max}\sum \alpha_i \exp(-k_i t) \tag{6}$$

The difference k_i and α_i were determined using quencher-free samples employing a multiexponential fit program. The most long-lived component gave k_0. In general, one or two exponentials were needed to describe the initial perturbation for which then the weight factors, α_i, were calculated using

$$\alpha_i = \frac{A_i}{\sum_i A_i} \tag{7}$$

where A_i is the amplitude for the different exponentials obtained from the fit. Using eq 6 in the evaluation allowed computer calculations much closer to zero time channel (ZTC) with retention of acceptable statistics and more reliable estimation of the parameters given in eq 3.

Results and Discussion

Binary PCMA−NaCl System. Figure 2a shows relaxation time distributions for PCMA in 1 mM NaCl. At this salt concentration the distributions are bimodal. Both relaxation rates are linearly dependent on the square of the scattering vector and pass through the origin showing that both modes are diffusive. The fast mode is attributed to the translation mobility of the single polyelectrolyte chain and the slow mode to multichain clusters (interpolyion association), a well-

known phenomenon existing in dilute polyelectrolyte solutions at low ionic strengths which has been discussed extensively in the literature.[26−33] The repulsion between fixed charges in the polyelectrolyte domains are long-ranged and give rise to a large excluded volume. Chain expansion leads to greater entanglement of the polyelectrolyte chains and formation of large aggregates, giving the slow relaxation modes.[34] Figure 2b shows that when the salt concentration is increased to 10 mM, the slow component disappears, a trend which is known for other polyelectrolytes in dilute solution, e.g. NaPSS.[27] At the same time, the scattered intensity increases owing to the more compact structure at higher salt concentrations and reduced overlap of the polycation molecules which change in conformation from a worm-like chain to a coil. Figure 2c illustrates the distribution of relaxation times for PCMA in 100 mM NaCl, corresponding to dimensions smaller than those at the two previous salt concentrations due to increased electrostatic screening of polyelectrolyte charges.

The concentration dependences of the diffusion coefficients, D, obtained from the relaxation rate of the fast mode (the single chain surfactant complexes) at three concentrations of added simple salt, are shown in Figure 2d. The concentration dependence of D is given by the relationship

$$D = D_0(1 + k_D C) \tag{8}$$

where D_0 is the infinite dilution diffusion coefficient and k_D is referred to as the hydrodynamic virial coefficient since it is in part related to the hydrodynamic interactions in the solution by $k_D = 2A_2M - k_f - 2\nu_2$. A_2 is the second virial coefficient, k_f describes the concentration dependence of the friction coefficient, f, and ν_2 is the partial specific volume of the solute. D_0 increases owing to a reduced R_h value. In the present case, $R_h = 60.1$, 47.7, and 45.8 nm in 10, 50, and 100 mM NaCl, respectively. Figure 2d contains a cross point at about 0.75 mM PCMA concentration. At this junction the effective diffusion coefficient for the polycation is independent of the NaCl concentration. At higher polyelectrolyte concentrations, D in 10 mM NaCl is higher than in 50 mM NaCl, i.e. the order is reversed compared with D_0 and is thus related both to the interaction potential and to the coil size. A summary of the DLS results is given in Tables 1a−c.

PCMA−SDS−NaCl System. Relaxation time distributions for the single-chain complex at an SDS/PCMA molar concentration ratio of 0.05 (mass concentration ratio 0.074) in 10 mM NaCl are shown in Figure 3a. Although the mass of the surfactant bound to the polyelectrolyte corresponds to only $^1/_{13}$th of the polyelectrolyte mass, the SDS micelles have a significant influence on the coil conformation. R_h for the complex, the faster mode, is substantially smaller than the surfactant-free dimension of the polymer at the same concentration of added NaCl. There is a parallel decrease in k_D for the complex; see Table 1. The interpretation placed on these results is that the surfactant reduces the charge density on the macroion, leading to coil contraction; this primary effect is reinforced by hydrophobic interaction, which in general is the main driving force in polymer−surfactant interactions. A slow component due to multichain clusters is present, which can also be seen in Figure 3b where the NaCl concentration is 50 mM. It is concluded that the cluster component is formed through charge interactions, as is the case for the surfactant-free polyelectrolyte at low ionic strengths since the slow mode in Figure 3c vanishes when the salt concentration is increased from 10 to 100 mM. Figures 3a−c show that the slow mode moves to shorter relaxation times when the simple salt concentration is increased, and at the same time, an increase in its amplitude is observed. The former effect indicates a transition from larger to smaller particles, and the latter a more compact structure with increased scattered intensity owing to the ionic strength increase. The single mode at 100 mM NaCl appears to be a combination between single-chain complex and incipient multichain structures.

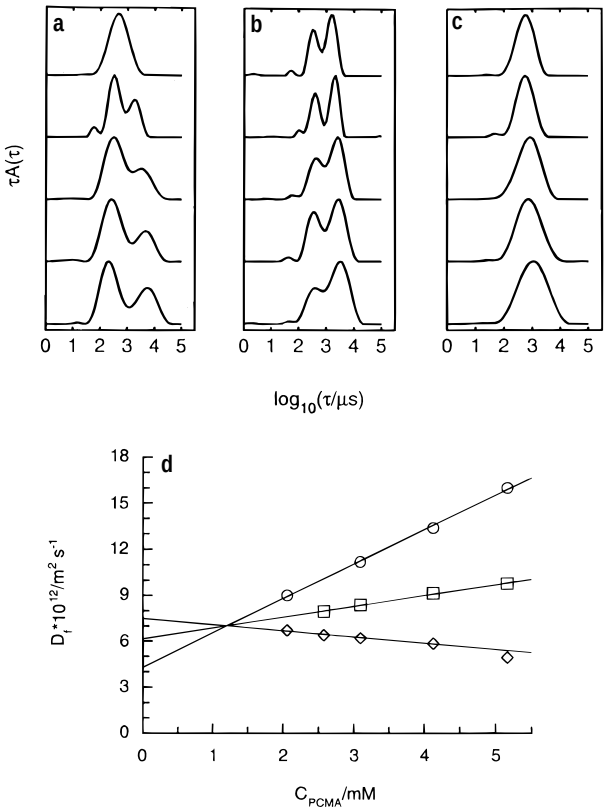

Figure 3. (a−c) Relaxation time distributions of PCMA−SDS complex with SDS/PCMA molar ratio 0.05. Concentrations of the polycation from top to bottom are 2.07, 2.58, 3.10, 4.13, and 5.16 mM, in (a) 10 mM NaCl, (b) 50 mM NaCl, and (c) 100 mM NaCl. (d) Effective diffusion coefficient, D, of the PCMA−SDS complex in 10 mM (○), 50 mM (□), and 100 mM NaCl (◇). SDS/PCMA = 0.05.

At low SDS concentrations in the present system, the solutions are optically clear. On increasing the SDS concentration the solution becomes turbid already at an SDS/PCMA molar ratio of ≈0.20 just prior to precipitation. This implies behavior different from that reported for a cationic-substituted cellulose ether and SDS between which a 1:1 complex was shown to be formed on the basis of charge neutralization.[35,36] The solubility characteristics of the complexes formed between polycations and anionic surfactants are complicated, and it has been shown that precipitation and subsequent resolubilization may be effected in some cases. The introduction of chain branches in the surfactant structure, for example, or of polyethoxy chains into the hydrophilic headgroup can drastically change the solubilization behavior.[37] The irreversible phase separation observed in the present system may be connected with the high charge density of the PCMA chain with one charge per monomer unit. Other polymer−surfactant systems which form insoluble complexes are poly(1-butyl-2-methyl-5-vinylpyridinium bromide) together with

Table 1. DLS Data

a. In 10 mM NaCl for the Fast and Slow Relaxation Modes

system	$10^{12}D_f$/m^2 s^{-1}	$R_{h,f}$/nm	$k_{D,f}$/L g^{-1}
PCMA	4.08	60.1	3.0
SDS/PCMA			
0.05	4.28	57.3	2.7
0.10	5.91	41.5	1.8
0.15	7.66	32.0	1.0
0.20	6.64	36.9	0.68
system	$10^{12}D_s$/m^2 s^{-1}	$R_{h,s}$/nm	$k_{D,s}$/L g^{-1}
SDS/PCMA			
0.05	1.04	236	−0.32
0.10	1.19	206	−0.42
0.15	1.41	174	−0.61
0.20	1.19	206	−0.45

b. In 50 mM NaCl for the Fast and Slow Relaxation Modes

system	$10^{12}D_f$/m^2 s^{-1}	$R_{h,f}$/nm	$k_{D,f}$/L g^{-1}
PCMA	5.14	47.7	0.92
SDS/PCMA			
0.05	6.15	39.9	0.60
0.10	7.08	34.6	−0.32
0.15	7.87	31.2	−0.64
0.20	4.84	50.7	−0.32
system	$10^{12}D_s$/m^2 s^{-1}	$R_{h,s}$/nm	$k_{D,s}$/L g^{-1}
SDS/PCMA			
0.15	1.67	147	−0.54
0.20	1.20	204	−0.41

c. In 100 mM NaCl

system	$10^{12}D$/m^2 s^{-1}	R_h/nm	k_D/L g^{-1}
PCMA	5.36	45.8	0.42
SDS/PCMA			
0.05	7.49	32.7	−0.28
0.10	7.79	31.5	−0.55
0.15	8.60	28.5	−0.73
0.20	4.13	59.4	−0.42

the soaps K caprate, K laurate, and K stearate,[38] and also with poly(vinyl sulfate)−cetyltrimethylammonium bromide (CTAB).[39]

The concentration dependences of D for the complexes formed at an SDS/PCMA molar ratio of 0.05 in 10, 50, and 100 mM NaCl are shown in Figure 3d. Increasing the NaCl concentration reduces the virial dependence of translational diffusion substantially, due to screening effects. The concentration dependence of D becomes negative in 100 mM NaCl solution. D_0 is larger and consequently R_h is smaller than in the lower salt concentrations.

The concentration dependencies of D corresponding to the single mode in the ILT curves from measurements in 100 mM NaCl are shown in Figure 4a, for the surfactant-free polymer and for the SDS/PCMA ratios 0.05, 0.10, 0.15, and 0.20. The magnitudes of D at finite concentrations are determined by the interplay between the thermodynamic property $(\partial\Pi/\partial C)$ and the friction coefficient f which is equal to $f_0(1 + k_fC)$. D_0 for the polycation is 5.36×10^{-12} m^2 s^{-1}. When SDS is added, D_0 becomes larger for the more compact structure and the virial dependence of D decreases as described above. The data in the figure corresponding to the ratio 0.20, the line for which deviates from the others, are attributed to the complex in the incipient turbid phase. At this ratio, the complex is close to the precipitation limit and aggregation occurs with hydrophobic interaction as the driving force. Large particles are formed, resulting in a smaller D_0 compared to values for the lower ratios.

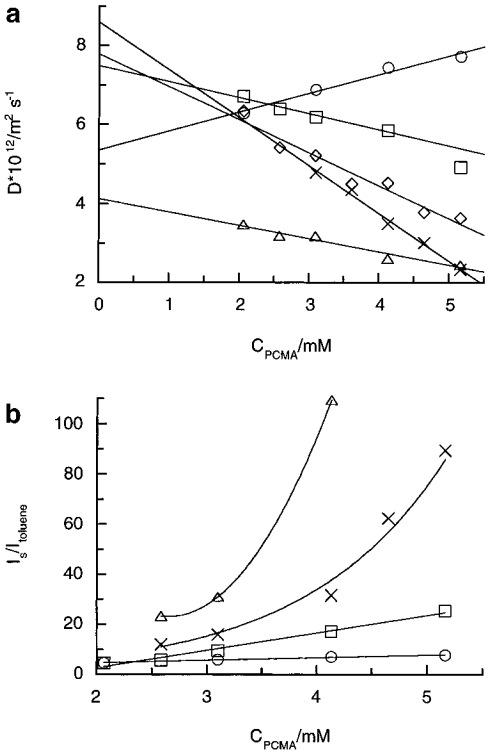

Figure 4. (a) Effective diffusion coefficient, D, as a function of polyelectrolyte concentration in 100 mM NaCl, for PCMA in the absence of SDS (○) and for SDS/PCMA = 0.05 (□), 0.10 (◇), 0.15 (×), and 0.20 (△). (b) Normalized time-average scattered intensity as a function of PCMA concentration in 100 mM NaCl, for PCMA in the absence of SDS (○) and for SDS/PCMA = 0.05 (□), 0.15 (×), and 0.20 (△).

The results in Figure 4b illustrate the total scattered intensity relative to toluene as a function of the polyion concentration, in 100 mM NaCl. The latter reinforce the results of the SDS/PCMA ratio dependence of D_0 shown in Figure 4a. There is only a modest increase in the total intensity with concentration increase for the two lowest curves, since no conformational transition of the polyion or the complex occurs. The increase in intensity is only due to a greater number of particles in the illuminated volume. Considering the two curves for the two highest ratios, the intensity increases considerably as a function of concentration, due to the formation of large particles.

R_h for the fast relaxational mode for the complex is shown in Figure 5a as a function of the SDS/PCMA molar concentration ratio in 10, 50, and 100 mM NaCl, respectively. When the ratio is increased the charge density on the chain is reduced, resulting in a decrease in R_h. Considering a fixed SDS/PCMA ratio, the decrease in R_h with increasing ionic strength is more pronounced at a lower SDS/PCMA ratio than at a higher ratio since in the former case the complex possesses a higher charge density which is influenced by screening by the salt.

k_D is depicted in Figure 5b as a function of surfactant/polyion ratio in 10, 50, and 100 mM NaCl, respectively. k_D decreases as a function of the ratio since the thermodynamic interaction between the complex and the solvent decreases when the system moves toward the saturation limit and precipitation. It should be emphasized that the value of k_D is negative in 50 and 100 mM NaCl at SDS concentrations close to saturation. This coefficient is related to the second virial coefficient A_2 and shows a similar variation as R_h and A_2 with an

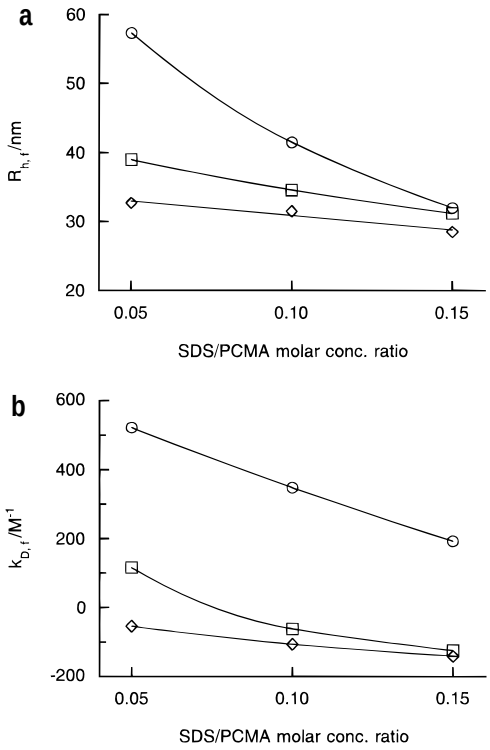

Figure 5. The hydrodynamic radius, R_h, of the complex as a function of the molar ratio SDS/PCMA in 10 mM (○), 50 mM (□), and 100 mM NaCl (◊). (b) Hydrodynamic virial coefficient, k_D, for the complex as a function of the SDS/PCMA ratio in 10 mM (○), 50 mM (□), and 100 mM NaCl (◊).

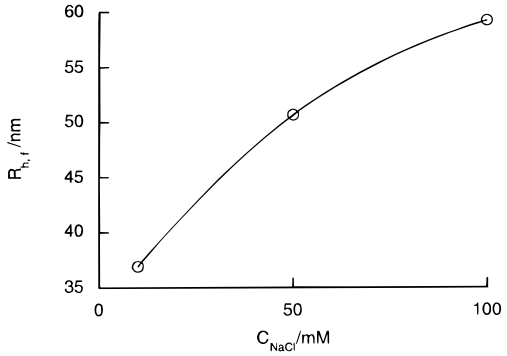

Figure 6. Hydrodynamic radius, R_h, of the fast relaxation mode at SDS/PCMA = 0.20, as a function of NaCl concentration.

increased binding of micelles to the polymer, a trend also reported earlier for the work on PEO−SDS interaction.[40]

Figure 6 shows how R_h for the complex in the incipient turbid phase (SDS/PCMA = 0.20) changes with NaCl concentration. The trend is opposite to that for the lower ratios, where R_h becomes smaller on addition of simple salt. Since the complex is close to phase separation at ratio 0.20, no further screening of charges occurs, which would result in a decrease in R_h. The increase in R_h with NaCl concentration shows that addition of salt at the saturation limit of the complex promotes the aggregation process.

Static Light Scattering Results. Figure 7a depicts a Zimm plot for the SDS/PCMA molar ratio 0.05 in 100 mM NaCl. The concentration C in (KC/R_θ) refers to the total concentration, i.e. the PCMA concentration plus the SDS concentration. The circles correspond to finite C values, in g mL^{-1}, of the complex at finite angles, and the squares correspond to the extrapolated data at zero concentration and zero angle. C was chosen within a well-examined concentration interval, the same as for the DLS measurements. R_g was determined as 79.2 nm and A_2 as 3.3×10^{-4} mol mL g^{-2}.

Figure 7b shows the Zimm plot for surfactant/polyion molar ratio 0.15, $R_g = 70.4$ nm, and $A_2 \cong -1.5$ mol mL g^{-2}. As seen in Tables 1 and 2, R_g and R_h change in the same manner as a function of bound SDS micelles as do the interaction parameters A_2 and k_D. The low net charge density of the complex at this neutralization degree is reflected in the negative, nonlinear concentration dependence of the reduced intensity.

The concentration dependencies of KC/R_θ at zero angle in 100 mM NaCl for the polyion and for the complex at different ratios are depicted in Figure 7c, where A_2 has been determined from the initial slopes. There is a strong decrease in A_2 with increasing SDS/PCMA ratio. The weight average molecular weights for the different ratios were not distinguishable because of small variations within the experimental error. Doty and Steiner[41,42] emphasized that there is an electrostatic interaction potential between segments of different polyelectrolyte chains. High polymer concentration and low ionic strength will lead to an ordering of particles in the solution with a subsequent reduction in scattered intensity for each polyelectrolyte chain. To avoid this interference, the concentrations have to be as low as possible. This effect leads to upward curvature of KC/R_θ as a function of polyelectrolyte concentration and was observed by Takahashi et al.[43] who studied NaPSS of various molecular weights in solutions of different ionic strengths. In Figure 7c, the curve fit for the polyion without surfactant is linear over the entire concentration range (0.04−0.10%). The deviations from linearity of the reduced intensity with regard to the PCMA−SDS mixtures at the higher concentrations are caused by the formation of large particles (see Figure 4b). This transition appears to be in its initial phase, since the field correlation function from the DLS measurements shows a single decay process.

Examples of the angular dependence of the total intensity are illustrated in Figure 7d for the SDS/PCMA ratio 0.15 at several concentrations. Extrapolation to zero concentration has been done over different q ranges. SLS results are summarized in Table 2.

Conformation of the PCMA Chain, the PCMA−SDS Complex, and Aggregates. The radii of gyration were calculated from the relation

$$\frac{KC}{R_{\theta,C=0}} = \frac{1}{M_w}\left(1 + \frac{q^2 R_g^{\,2}}{3}\right) \qquad (9)$$

and compared to those calculated from the angular dependence of the internal structure factor $P(X)$ for a Gaussian coil, with $X = qR_g$. For different scattering vectors at zero concentration, the internal structure factor $1/M_w(KC/R_\theta)^{-1}$ satisfies the function $P(X) = 2/X^4$-$[\exp(-X^2) + X^2 - 1]$. The radii of gyration obtained from this function agreed with those determined from the slopes of the angular dependence in the Zimm plots in the chosen q ranges. At low ionic strengths, the structure would resemble that of a wormlike chain owing to a stronger Debye−Hückel potential between the polyion segments. At an SDS/PCMA ratio of 0.05, partial charge neutralization leads to a more compact Gaussian coil, an effect which becomes larger as the neutralization degree is increased. Since the concentration dependence of D decreases and eventually becomes

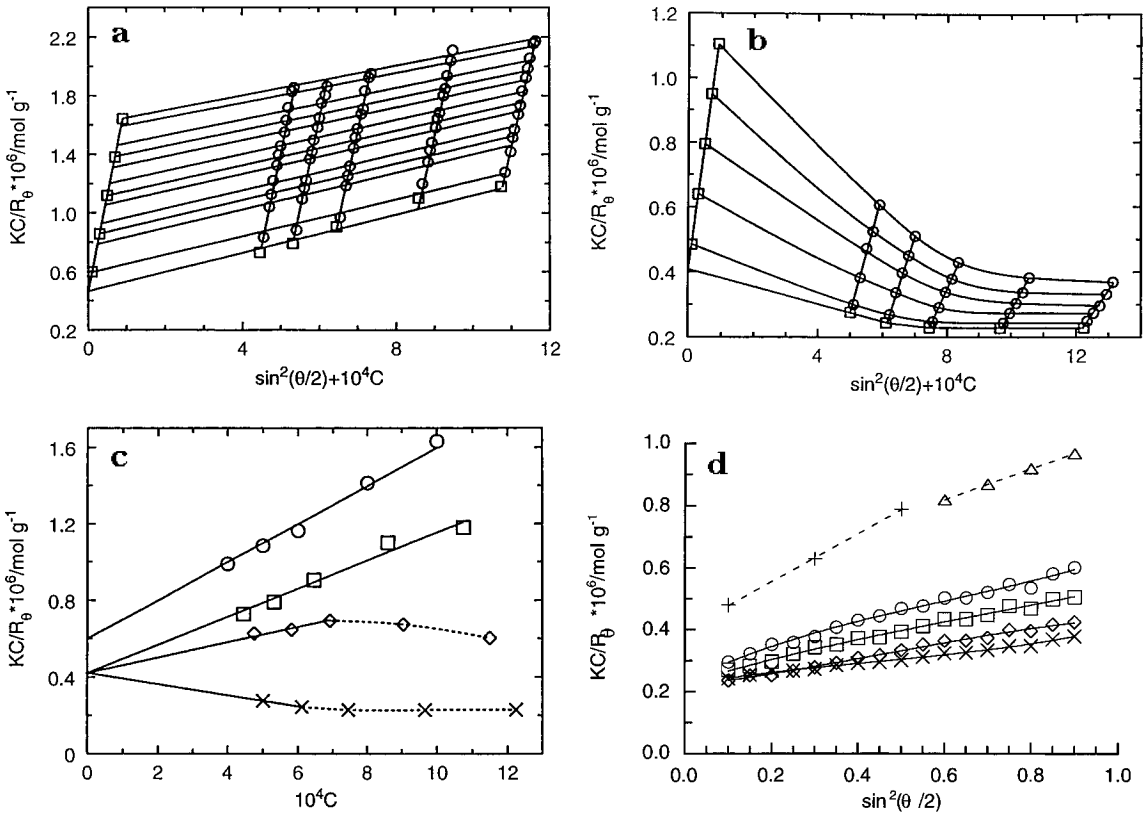

Figure 7. (a) Zimm plot for the surfactant/polyion molar ratio 0.05 in 100 mM NaCl. The concentrations of the polyion are 0.04, 0.05, 0.06, 0.08, and 0.10%. (b) Zimm plot for the surfactant/polyion molar ratio 0.15 in 100 mM NaCl. The concentrations of the polyion are 0.04, 0.05, 0.06, 0.08, and 0.10%. (c) Reduced scattered intensity as a function of the concentration of the PCMA−SDS complex at zero angle. At the top is PCMA in the absence of SDS (○), succeeded by the SDS/PCMA ratios 0.05 (□), 0.10 (◊), and 0.15 (×). (d) Examples of the angular dependence of KC/R_θ, related to the internal structure factor. SDS/PCMA = 0.15 in 100 mM NaCl. The finite concentrations of PCMA are 0.04 (○), 0.05 (□), 0.06 (◊), and 0.08% (×). The symbols + and Δ are values extrapolated to infinite dilution, in two different q ranges.

Table 2. SLS Data and Specific Refractive Index Increments in 100 mM NaCl

	R_g/nm			
system	high q range	low q range	10^4A_2/mol mL g^{-2}	$\partial n/\partial C$/mL g^{-1}
PCMA	84.6	128	5.0	0.163
SDS/PCMA				
0.05	79.2	110	3.3	0.137
0.10	74.2	94	2.0	0.126
0.15	70.4	91	−1.5	0.110

negative with increasing SDS/PCMA ratio, it is clear that the polyelectrolytic character of the complex decreases as a function of SDS concentration. Polyelectrolyte−surfactant association probably results in localization of the PCMA chains in the micellar headgroup region with formation of a more compact structure for the complex than the single polymer coil. The polyion−surfactant complex formation has a greater influence on the conformation than does screening by a simple salt, owing to reinforcement of the interactions by hydrophobic effects. A similar effect was observed in the system NaPSS−CTAB.[13]

The clusters arising on interpolyion association appear to be electrostatically stabilized in PCMA solutions when SDS is present since they vanish when the NaCl concentration is increased. On the other hand, the clusters formed in the NaPSS system when CTAB is present are apparently hydrophobically stabilized since an increase in salt concentration enhances the aggregation when the free polyelectrolyte charges are screened. This may be due to the relatively high neutralization degrees in the latter case, implying a large number of hydrophobic domains in the system. Sections a and b of Table 1 give the hydrodynamic radii of the slow relaxation mode (the clusters) at different SDS/PCMA molar concentration ratios in 10 and 50 mM NaCl. In 10 mM NaCl, R_h for the slow mode decreases from 236 to 174 nm when the SDS/PCMA ratio is increased from 0.05 to 0.15. At the ratio 0.20 the trend reverses and the size increases again. The initial decrease in R_h with increasing SDS concentration is due to electrostatic and hydrophobic interactions between the polyelectrolyte and the micelles. Multichain clusters are probably formed by more than one chain being associated with a given surfactant micelle, i.e. the structure resembles an incipient network in comparison with the pure PCMA solution. At the highest ratio of 0.20 on the other hand, R_h = 206 nm, i.e. a larger value, as might be anticipated close to phase separation when the cluster size increases. The proportion of multichain aggregates increases at this point because a greater number of micelles serve as junctions for the polyelectrolyte chains. In 50 mM NaCl, the hydrodynamic radii are smaller than in 10 mM, implying that electrostatic screening has an influence even on the slow relaxation mode.

Surface tension measurements were carried out at a constant PCMA concentration of 0.06% in 50 and 100 mM NaCl, resulting in cac values of 0.15 and 0.12 mM SDS respectively, as depicted in Figure 8. This observation implies that the stabilization of the complex is greater in 100 mM than in 50 mM NaCl. Usually, an increase in simple salt concentration leads to an increase in the cac for oppositely charged polyelectrolytes and surfactants; i.e. the salt reduces the electrostatic

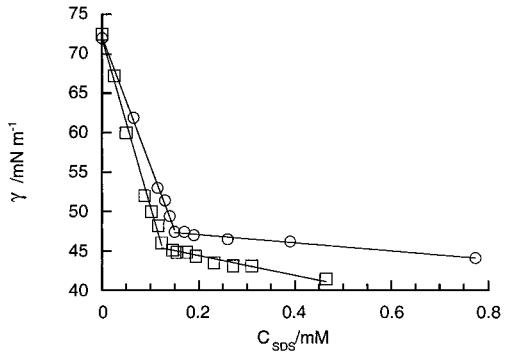

Figure 8. Surface tension, γ, as a function of SDS concentration with PCMA concentration held constant at 3.10 mM (0.06%), in 50 mM (○) and 100 mM NaCl (□).

Table 3. Pyrene Fluorescence Lifetimes, Surfactant Aggregation Numbers, and Quenching Rate Constants from Time-Resolved Fluorescence Quenching Measurements

SDS/PCMA ratio	C(NaCl)/mM	τ_0/ns[a]	N_{agg}[b]	$10^{-6}k_q/s^{-1}$	χ^2
0.15	50	317	174	3.7	1.08
0.20	50	322	192	3.6	1.20
0.05	100	318	184	4.0	1.08
0.15	100	324	208	3.9	1.19
0.20	100	324	225	3.5	1.14

[a] Measured at 25 °C. All samples were deoxygenated using freeze−thaw cycles. [b] From TRFQ measurements at 25 °C, with pyrene as probe and DMBP as quencher. The pyrene concentration was below 0.1 μM, and the quencher to surfactant ratio ranged from 0.003 to 0.009.

attraction between the micelles and the polyion. At high salt concentrations the bound surfactant micelles are stabilized, as indicated by a decrease in the cac. It seems that this system is governed by the latter of these two effects when the NaCl concentration is increased from 50 to 100 mM.

Time-Resolved Fluorescence Quenching Results. The surfactant aggregation numbers, N_s, fluorescence lifetimes of pyrene monomer emission, τ_0, and the dynamics of the quenching process reflected in the first-order quenching rate constant, k_q, obtained from fitting to the model given in eq 6 are presented in Table 3. Representative TRFQ decay data are shown in Figure 9a for a sample with and without DMBP composed of 3.10 mM PCMA (0.06%) and 0.465 mM SDS in 50 mM NaCl. Figure 9b shows typical weighted residuals obtained from fitting to the generalized model with correction for the impurity fluorescence. The goodness of the fitting procedure is given by the χ^2 values and the autocorrelation of weighted residuals. In the determination of the aggregation numbers using eq 4, the amount of surfactant participating in the complex formation is taken as the difference between the total surfactant concentration and the cac, as determined from the surface tension measurements above, assuming that all bound surfactant is in the micellar form. For an accurate estimation of N_s, knowledge of the quencher distribution between the bound micellar subphase and the aqueous phase is required. A precise determination of the distribution constant was not made, but instead it was assumed that the quencher is distributed in a way similar to that found in the case of pure SDS micelles at 25 °C. The final concentration of quenchers in the hydrophobic micellar phase was therefore calculated using the distribution constant for DMBP between the micellar subphase and aqueous phase as 2994 M^{-1} estimated for pure SDS micelles.[44]

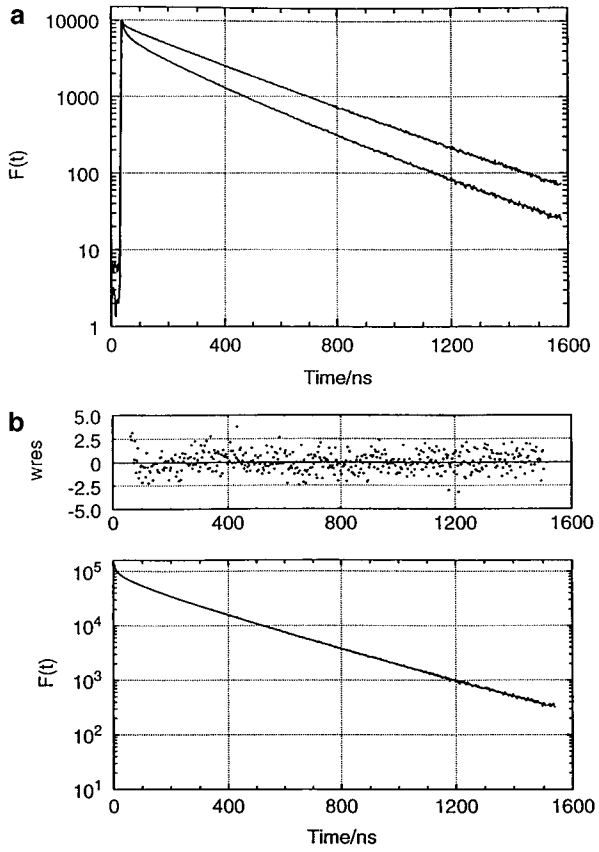

Figure 9. (a) Time-resolved fluorescence decay curves for a sample with 3.10 mM PCMA (0.06%) and 0.465 mM SDS in 50 mM NaCl. Unquenched and quenched samples from the top. (b) Curve fit for the quenched fluorescence decay in Figure 9a (lower) and the corresponding residuals (upper).

N_s values estimated in 50 mM NaCl at SDS/PCMA ratios of 0.15 and 0.20 are 174 and 192, respectively. In 100 mM NaCl, N_s = 184, 208, and 225 at the ratios 0.05, 0.15, and 0.20, respectively. In all cases the N_s values are close to or larger than twice the value found for SDS micelles in the absence of polymer under identical conditions. N_s = 90 was reported for SDS micelles in 100 mM NaCl in the absence of polymer.[45] It is the normal trend that N_s increases as a function of surfactant concentration within the two series. This increase is also observed when more salt is added to the system because of the reduced electrostatic interaction between the surfactant headgroups at the micellar curvature. k_q does not show any significant trend but is similar for the different compositions; the values are, however, much lower than those found for SDS micelles without PCMA, suggesting that the mobilities of the probe and quenchers are strongly reduced in the bound micelles. This result is also consistent with the larger size of the bound micelles. From the individual concentrations of polyelectrolyte and surfactant micelles in the PCMA−SDS mixtures and the aggregation numbers of the bound micelles, the average number of SDS micelles per chain in 100 mM NaCl was estimated to be 0.6 and 7.4 at the SDS/PCMA ratios 0.05 and 0.20. The possible association of more than one polyelectrolyte chain with a given micelle has not been taken into account. Seven micelles per chain corresponds to a transition in the system from an optically clear solution to a turbid phase.

Conclusions

R_h of the PCMA−SDS complex is smaller than that for the polyelectrolyte in the absence of surfactant, as a result of a combination of electrostatic and hydrophobic interactions. At low ionic strengths, two components of dissimilar size are present, where the smaller component is attributed to the single-chain PCMA−SDS complex and the larger component to an electrostatically stabilized cluster involving several polyion chains which are cross-linked through the micelles. A decrease in R_g is observed as the SDS/PCMA ratio is increased, in agreement with the changes in R_h. The concomitant reduction in A_2 when the SDS/PCMA ratio is increased reflects the decline in the interaction potential when the complex approaches phase separation. The aggregation numbers of the polyelectrolyte-bound micelles at different SDS/PCMA ratios are larger than those for SDS in the absence of PCMA at the same concentrations of NaCl.

Acknowledgment. Per Claesson and Mats Dahlgren at the Royal Institute of Technology in Stockholm are thanked for interesting discussions and for the supply of PCMA. This work has been supported by the Swedish National Board for Technical Development (NUTEK) and the Swedish Technical Research Council (TFR).

References and Notes

(1) Jones, M. N. *J. Colloid Interface Sci.* **1967**, *23*, 36.
(2) Schwuger, M. J. *J. Colloid Interface Sci.* **1973**, *43*, 491.
(3) Shirahama, K. *Colloid Polym. Sci.* **1974**, *252*, 978.
(4) Cabane, B. *J. Phys. Chem.* **1977**, *81*, 1639.
(5) Breuer, M. M.; Robb, I. D. *Chem. Ind.* **1972**, 530.
(6) Jones, M. N. *J. Colloid Interface Sci.* **1968**, *26*, 532.
(7) Cabane, B.; Dupplesix, R. *Colloids Surf.* **1985**, *13*, 19.
(8) Francois, J.; Dayantis, J.; Sabbadin, J. *Eur. Polym. J.* **1985**, *21*, 165.
(9) Witte, F. M.; Engberts, J. B. F. N. *Colloids Surf.* **1989**, *36*, 417.
(10) Holmberg, C.; Nilsson, S.; Singh, S.; Sundelöf, L.-O. *J. Phys. Chem.* **1992**, *96*, 871.
(11) Hayakawa, K.; Kwak, J. C. T. *J. Phys. Chem.* **1982**, *86*, 3866.
(12) Abuin, E. B.; Scaiano, J. C. *J. Am. Chem. Soc.* **1984**, *106*, 6274.
(13) Fundin, J.; Brown, W. *Macromolecules* **1994**, *27*, 5024.
(14) Dubin, P. L.; Oteri, R. *J. Colloid Interface Sci.* **1983**, *95*, 453.
(15) Macdonald, P. M.; Staring, D.; Yue, Y. *Langmuir* **1993**, *9*, 381.
(16) Mabire, F.; Audebert, R.; Quivoron, C. *Polymer* **1984**, *25*, 1317.
(17) Mukerjee, P.; Mysels, K. J. *Critical Micelle Concentration of Aqueous Surfactant Systems*; NSRDS-NBS 36; National Bureau of Standards: Washington, DC, 1971.
(18) Nicolai, T.; Brown, W.; Johnsen, R. M.; Štěpánek, P. *Macromolecules* **1990**, *23*, 1165.
(19) Jakeš, J. *Czech. J. Phys.* **1988**, *B38*, 1305.
(20) Provencher, S. W. *Macromol. Chem.* **1979**, *180*, 201.
(21) Pike, E. R.; Pomeroy, W. R. M.; Vaughan, J. M. *J. Chem. Phys.* **1975**, *62*, 3188.
(22) Almgren, M.; Hansson, P.; Mukhtar, E.; van Stam, J. *Langmuir* **1992**, *8*, 2405.
(23) Infelta, P. P.; Grätzel, M.; Thomas, J. K. *J. Phys. Chem.* **1974**, *78*, 190.
(24) Almgren, M.; Löfroth, J.-E.; van Stam, J. *J. Phys. Chem.* **1986**, *90*, 4431.
(25) Tachiya, M. *Chem. Phys. Lett.* **1975**, *33*, 289.
(26) Lin, S. C.; Lee, W. I.; Schurr, J. M. *Biopolymers* **1978**, *17*, 1041.
(27) Drifford, M.; Dalbiez, J.-P. *Biopolymers* **1985**, *24*, 1501.
(28) Foerster, S.; Schmidt, M.; Antonietti, M. *Polymer* **1990**, *31*, 781.
(29) Sedlák, M.; Konák, C.; Štěpánek, P.; Jakes, J. *Polymer* **1987**, *28*, 873.
(30) Zero, K.; Ware, B. R. *J. Chem. Phys.* **1984**, *80*, 1610.
(31) Schmitz, K. S.; Ramsay, D. J. *Biopolymers* **1985**, *24*, 1247.
(32) Sedlák, M.; Amis, E. J. *J. Chem. Phys.* **1992**, *96*, 817.
(33) Reed, W. F. *Macromolecules* **1994**, *27*, 873.
(34) Sedlák, M.; Amis, E. J. *J. Chem. Phys.* **1992**, *96*, 826.
(35) Goddard, E. D.; Phillips, T. S.; Hannan, R. B. *J. Soc. Cosmet. Chem.* **1975**, *26*, 461.
(36) Goddard, E. D.; Hannan, R. B. *J. Colloid Interface Sci.* **1976**, *55*, 73.
(37) Goddard, E. D.; Hannan, R. B. *J. Am. Oil Chem. Soc.* **1977**, *54*, 561.
(38) Aleksandrovskaya, S. A.; Tretýakova, A. Ya.; Barabanov, V. P. *Vysokomol. Soedin. Ser. B* **1984**, *26*, 280.
(39) Harada, A.; Nozakura, S. *Polym. Bull.* **1984**, *11*, 175.
(40) Brown, W.; Fundin, J.; da Graça Miguel, M. *Macromolecules* **1992**, *25*, 7192.
(41) Doty, P.; Steiner, R. F. *J. Chem. Phys.* **1949**, *17*, 743.
(42) Doty, P.; Steiner, R. F. *J. Polym. Sci.* **1950**, *5*, 383.
(43) Takahashi, A.; Kato, T.; Nagasawa, M. *J. Phys. Chem.* **1967**, *71*, 2001.
(44) Alsins, J. Private communication.
(45) Lianos, P.; Zana, R. *J. Phys. Chem.* **1980**, *84*, 3339.

MA950510R